J Mater Sci (2007) 42:6642–6650
DOI 10.1007/s10853-007-1520-2

Impact response of composites after long-term water immersion

Kyriakos Berketis · P. J. Hogg

Received: 27 March 2006 / Accepted: 16 January 2007 / Published online: 1 May 2007

Abstract Woven and non-crimped glass fabric reinforced polyester flat composite plates are studied experimentally. Water immersion tests for undamaged and impact damaged specimens are performed. The accelerating effects of increased water temperature on the degradation rate are discussed. The effect of up to 30 months water immersion on the impact behaviour are extensively investigated and compared with pre-water immersion results. The effects of different E-glass fabric reinforcement types, woven and non-crimped, in terms of environmental and impact behaviour are reported. An Environmental Damage Accumulation Metric (EDAM) is proposed and analysed, linking the time of water immersion with a marked change of behaviour in terms of the loss of the elastic component during the impact event.

Introduction

The effects of aqueous immersion on composites although studied extensively [1–3] are still a subject of practical interest that cannot be classified as resolved. Water immersion is known to have different effects depending on the composite constituents, i.e., the matrix [4, 5] and fibres used [6], the condition of the interface [7], the processing route employed [8] at the manufacturing stage. To follow the degradation process at room temperature would be very slow and for this reason nearly all studies employ an accelerating factor to bring the observation time within practical acceptable levels. Most usually accelerated degradation tests are performed by increasing the temperature of the exposure media [9]. For GFRP based on polyester resin, water immersion up to the boiling point has been reported [10]. Increasing the temperature of immersion could initiate secondary effects that cause irreversibility to the water absorption profile [11].

Knowledge of the water absorption behaviour of a class of resins within the polyesters group does not necessarily help predicting the behaviour of a particular type of commercial polyester, which is normally a mixture of individual types of pre-polymers. Simplistic approaches such as by the use of the rule of mixtures are not necessarily, valid [12]. Still the main tool of study of water immersion effects is long-term accelerated and ambient temperature observation of the water absorption/de-sorption.

Barely visible low velocity impact damage can be introduced to composite components and structures in situations such as those encountered by a falling tool or in a collision with a floating item in the marine environment. The damage caused by the out of plane impact can result in a serious reduction of the in-plane mechanical properties of laminate composites. The subject of impact on composites and the results of impact on the residual mechanical properties have been extensively studied over the years [13–16]. The complex loading state encountered during impact has not allowed yet for a universally applicable model that predicts the initiation and propagation of damage [17].

Work on the combined effects of water immersion and impact [18–20] is somewhat scarce due to the difficulty in assessing the end result. No direct link between the study of water absorption profiles and changes in the mechanical behaviour characteristics has been found. It is as the

K. Berketis (✉) · P. J. Hogg
Materials Department, Queen Mary, University of London, Mile End Road, London E1 4NS, UK
e-mail: k.berketis@qmul.ac.uk

phenomena are studied in parallel and their respective timelines do not intersect. The mechanisms of the individual processes of impact and water absorption are generally understood but their interaction not yet clearly. The study of the interaction should be the long-term goal.

Materials, fabrication and testing

Three E-glass/polyester panels each measuring $1{,}300 \times 1{,}000$ mm^2 were provided by Vosper Thorneycroft. The material was manufactured by the vacuum assisted resin transfer moulding (VARTM) technique. For the manufacture of all plates used in this project, the isopthalic polyester resin Crystic 489 PA, produced by Scott Bader, was used. One balanced plain woven glass, for material marked A and two non-crimped fabric types for materials type B and D were used for the plates. The lay-up of the three material types along with details of the fabric types used are presented in Table 1.

Neat resin has been cast in a plate mould to create 3 mm thick plates for water absorption experiments. Three specimens from neat resin and three specimens from each composite plate type were cut at 45×45 mm^2 for water absorption tests. The cut specimens have been post-cured for 3 h at 80 °C. The edges of the specimens have been covered with Hysol XEA 9359.3 QT epoxy adhesive to minimise diffusion through the specimen edges. These specimens were positioned in 1 L sealed glass containers spaced so that the specimens did not touch each other. The containers were immersed in thermostatically controlled, stainless steel lined baths manufactured by Grant. The temperature controller was capable of ± 0.1 °C.

For water absorption results with plates containing impact damage, four specimens of each material type at any impact energy level, including no impact damage, with dimensions 55×89 mm^2 were used. In this case the edges of the specimens were not sealed. These sets of specimens were rested on stainless steel racks and immersed in the water baths.

Composite plates were immersed in deionized water at 43 °C, a temperature higher than ambient but accepted for continuous use for a composite made from this resin system. A higher immersion temperature of 65 °C was also used that was expected to significantly accelerate the degradation process but in the short-term the effects would not be detrimental. Results from further tests performed at 93 °C can be found in [21].

An Ohaus Explorer, temperature compensating digital scales with accuracy of ±0.0001 g was used for weight uptake measurements. Specimens were taken out of the baths and their surface was dried of the excess water with paper towels before placing on the weighing pan. Specimens taken out from the 65 °C baths were weighed as fast as possible, because the scales reading did not reach a stable level as there was continuous evaporation from the specimens.

The glass fibre volume fraction of the materials under study has been determined by the resin burn-off technique, as per ASTM D2583. The results of the measurement are presented in Table 2.

Impact damage was introduced for some of the panels before and for some after water immersion. A range of three levels of impact energy have been used, namely 2.5, 5 and 10 J. Four specimens were impacted at each impact energy level. The minimum impact energy level was selected so that the force registered would be above the Delamination Threshold Load [17] for all three types of material available. This was expected to be a cause of subsequent reduction in the in-plane mechanical properties and more specifically when loading in compression. The maximum impact energy level was chosen so as not to cause penetration damage to dry specimens and also so that the damaged area's maximum diameter would not reach the size of the clamping window frame used, whose diameter was 40 mm. If the latter happened the real extent of the damage could have been restricted and the damage patterns changed by the clamping arrangement.

Specimen plates were pneumatically clamped with a pressure of 7 bars, from top and bottom between a pair of steel plates. These plates had a 40 mm diameter window on their centres and the striker was of hemispherical shape with a 10 mm radius. Figure 1 depicts the arrangement of the test clamping conditions.

Thickness variations between different specimens of the same material types were not compensated with different height or weight adjustments of the striker. The drop height and therefore the terminal velocity were kept constant at 2.83 m/s and weights were added to the striker sleigh to increase the initial impact energy.

Table 1 The material types used according to the fibre fabric architecture reinforcement and the name used to refer to them in the project

Plate name	Fabric type	Weave type	Lay-up
A	Chomarat 600T	Balanced plain woven	$(0°,90°)_6$
B	Cotech EBX-602	Biaxial NCF	$(\pm45°)_6$
D	Cotech EBX-602, Cotech ETLX-1169	Biaxial NCF, triaxial NCF	$(\pm45°,0°),(\pm45°)_2,(0°,\pm45°)$

Table 2 Density ρ_c, fibre volume fraction V_f and void content V_v results for all material types after resin burn-off

Material type	ρ_c	V_f (%)	V_v (%)	Average plate thickness
A	1.85	49.57	0.27	3.00
B	1.73	42.07	0.32	3.50
D	1.70	38.52	0.33	3.88

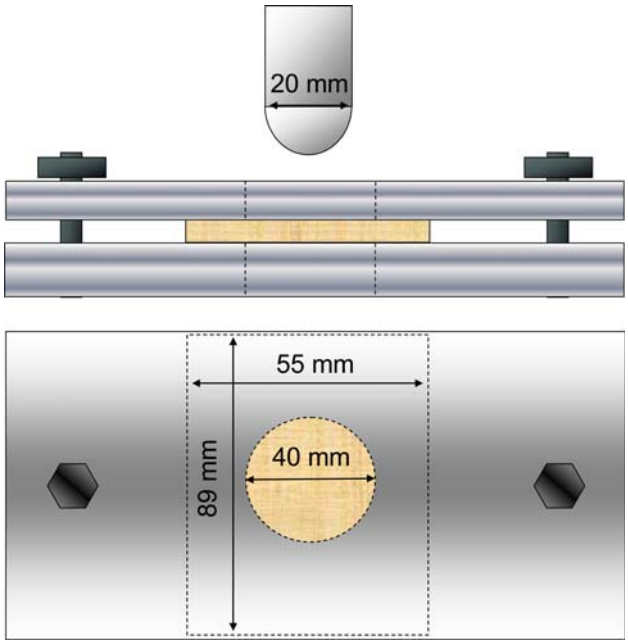

Fig. 1 A schematic of the arrangement of the striker and the plates holding the specimen for impact

Results

Water immersion results

The results of the weight change of the composite plates with respect to time, after water immersion at the temperatures of 43 and 65 °C are presented in Fig. 2a, b, respectively.

Some sets of specimens were impacted and immersed in water in order to study the relative effect of damage on water absorption. The sets of specimens used were impacted at 2.5, 5 and 10 J. The initial damage size was recorded by digital photographs. Based on the assumption that the relative ranking in terms of water uptake would agree with the small specimens results presented above not all materials in all temperatures were tested. The results are presented in Fig. 3.

Damage caused by low velocity impact normally takes the form of delaminations, matrix cracks, fibre debonding and breakage. Pre-existing damage on the plates could lead to higher absorption rate and possibly a higher saturation level, as more paths are available for diffusion. From Fig. 3a, results at 43 °C, some remarks can be made regarding the uptake rate and the saturation level. The resin specimens clearly reach a higher saturation level within the test time. Damage seems to have an effect on the saturation level at this temperature as specimens impacted at 5 and 10 J group separately from the specimens with no damage or impact at 2.5 J. The small size of damage caused by the 2.5 J impact does not allow for large discrepancies from the undamaged specimen.

At 65 °C, Fig. 3b, the role of damage caused by impact seems to be reduced, with only the heavily damaged with 10 J, B type specimens showing trends of higher absorption compared to the rest. This could signify that the swelling caused by water absorption is fast enough to act as an effective crack closure method. A similar case has also been reported by Lundgren and Gudmundson [22]. For the resin specimens the curve is different. At this temperature the resin is susceptible to microcracking, as shown in Fig. 4. Small cracks have been observed to form near the surface and inside the material. The density of cracks increased with time, reaching a level where light transmission was not effective for observation. The rate of formation of these cracks could allow for the explanation of both the sudden increase in water uptake, when compared to reinforced specimens, and the abrupt weight loss. It also seems that an incubation time exists between the formation and the activation of the cracks.

At 65 °C after ~14 months of water immersion a peak is observed in Fig. 2b followed by substantial drop in weight change percentage. The peak does not necessarily represent the maximum water absorption limit but signifies the point where the matrix degradation process becomes dominant. At 43 °C no peak point was found within the experimental observation limits. It remains unclear if such a pronounced peak would be found at this temperature.

Impact results before water immersion

Impact test results of specimens impacted prior to water immersion are presented here. Typical force–displacement curves from the three different material types are presented in Fig. 5.

The impact energies used are low enough to assume that linear elastic loading takes place. This assumption is tested using the energy balance equation [13] and assuming small

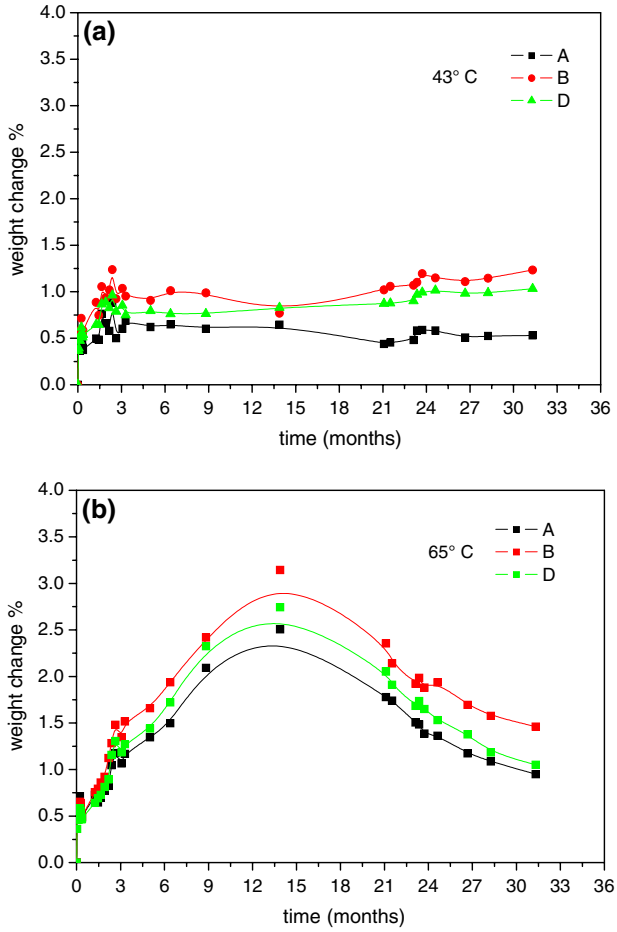

Fig. 2 In (**a**) and (**b**) the results from low (43 °C) and medium (65 °C) temperature water immersion, respectively, are presented for all material types with sealed edges

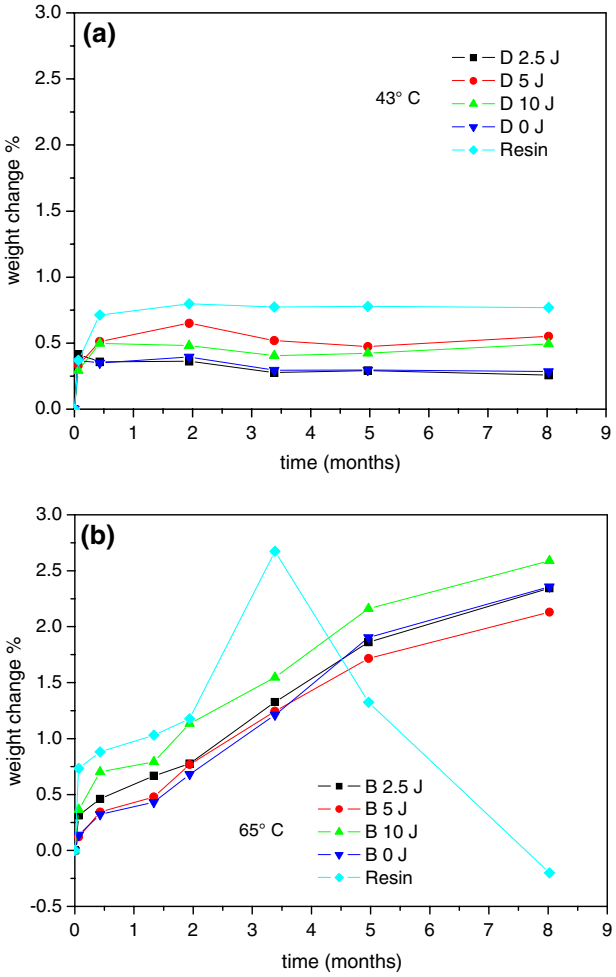

Fig. 3 Weight change after immersion in water at 43 °C for material type D in (**a**) and for material type B at 65 °C in (**b**). Specimens marked with 2.5, 5 and 10 J, respectively, have been impacted prior to immersion. Specimens marked 0 J were not impacted

deflections for the given material types and clamping conditions used, the peak force measured is plotted vs. the given impact energy in Fig. 6.

From Fig. 6 can be seen that there is a very good agreement for the first two energy levels of 2.5 and 5 J and only slight deviation for the 10 J impact level. The upwards deviation at 10 J from the square root relation can be due to increased membrane stresses due to larger deflections that are not accounted for using the assumed linear elastic loading conditions.

For graphs of energy absorption below the penetration limit, as in Fig. 7, with respect to time, energy increases up to the maximum and then when the striker rebounces as the plate recovers its initial position the energy reduces by an amount equal to the energy returned to the striker to rebounce. The plots of force vs. time in Fig. 7 also allow determining the Delamination Threshold Load (DTL) [17] point easier than in the case of force–displacement plots.

The closed area under the force displacement curve provides a measure of the absorbed impact energy. In order

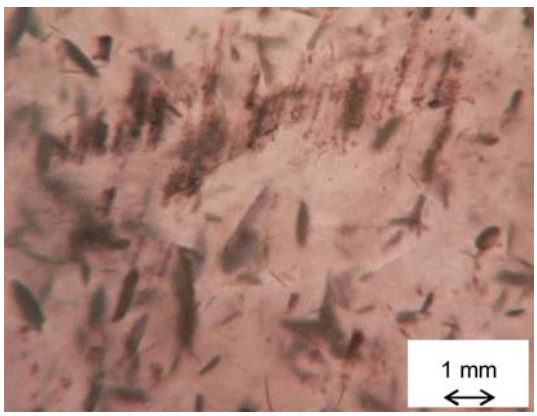

Fig. 4 Optical micrograph of neat resin plate microcracking after water immersion at 65 °C for 84 days

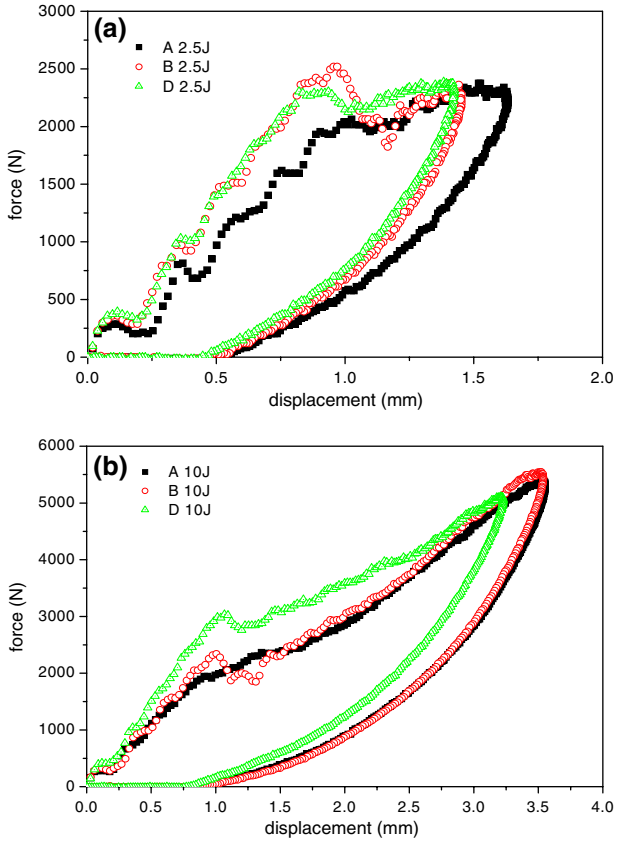

Fig. 5 Force–displacement response of dry impacted plates of all three types A, B and D for impact of 2.5 J in (**a**) and 10 J in (**b**)

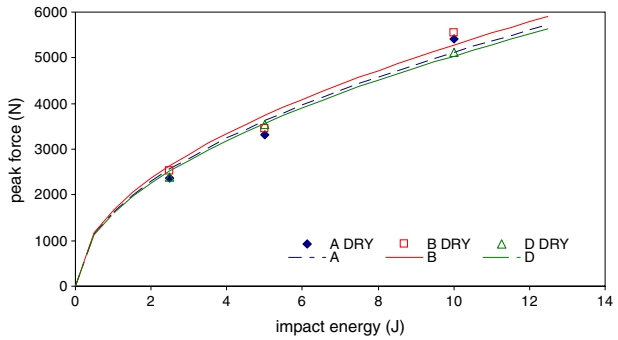

Fig. 6 Peak force with respect to impact energy. Lines represent the assumed square root relation

for the materials response, in terms of energy absorption, to be directly comparable, normalization against a common nominal thickness and fibre volume fraction is needed. An assumption is made that within the range of impact energies studied here specimen variations in thickness and glass volume fraction would follow a linear relationship with respect to absorbed energy. The normalization is performed against a plate thickness of 3.5 mm, and a fibre volume fraction of 43.4%, the average of the three materials. The calculation is performed as follows:

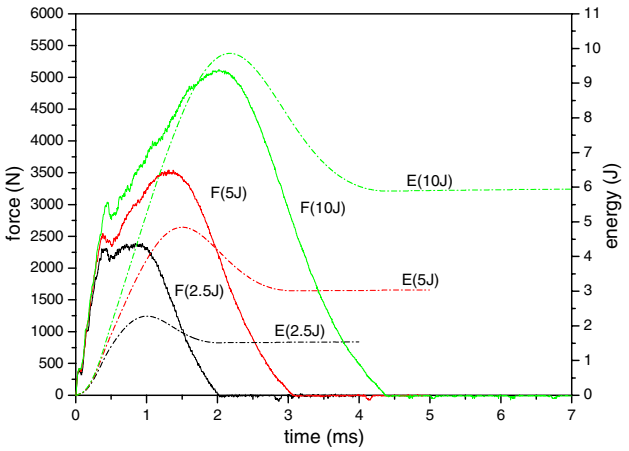

Fig. 7 Force–time F as solid lines and energy–time E as dotted lines for material type D at 2.5, 5 and 10 J impact energy levels

$$E_{\mathrm{n}} = E_{\mathrm{a}} \cdot \left(\frac{3.5}{t}\right) \cdot \left(\frac{V_{\mathrm{f}}}{43.4}\right), \tag{1}$$

where E_{n} is the normalized absorbed energy, E_{a} is the absorbed energy, t is the plate thickness, V_{f} is the fibre volume fraction of the specimen.

The normalized impact energy absorption results are plotted on Fig. 8. Linear fits of the results have also been performed on the same graph. The calculated parameters are shown on Table 3.

The slope of these lines is an indicator of the energy absorption ability of each of these materials. From the results the type A material with the woven fabric reinforcement shows much higher energy absorption compared to the two NCF reinforced material types. The y-axis intercept value, at 0 J impact energy is not zero for any of the materials. The values though are very near to the origin so

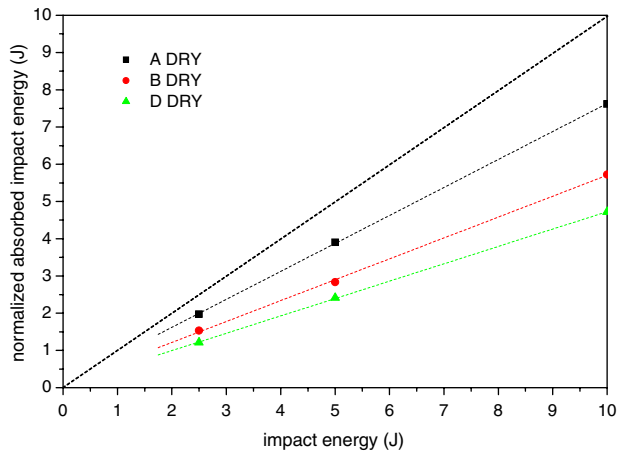

Fig. 8 Normalized absorbed impact energy for all material types impacted in dry condition marked as DRY. Dotted lines represent linear fit. The diagonal represents the penetration limit

Table 3 Linear fit results for A, B, D type materials for normalized impact energy absorption

	Slope	Intercept
AREF	0.75	0.12
BREF	0.56	0.09
DREF	0.47	0.06

they can be regarded as experimental error related to the use of nominal impact energy rather than actual impact energy for the graphs and the fitting.

Impact results after water immersion

The impact behaviour of plates after water immersion changes significantly as a function of time of immersion. The change exhibited by specimens over the test duration of 30 months is exhibited in Figs. 9, 10.

Assuming that within the range of impact energies tested, for any material type at any condition before and after water immersion, linear monotonic increase relationship exist between the energy absorbed and the impact energy, plots of the form $y = a + bx$ have been produced, representative examples can be seen in Fig. 11. The parameters a, the y-axis intercept and b the slope have been found using curve fitting.

The change of value of the energy absorption ratio parameter b can be used to characterize the condition of the material for impact before and after water exposure. Initially there is a large increase in energy absorption and gradually this trend eases, with respect to time of immersion. This is exemplified in Fig. 12.

The slope, parameter b has been used to define an Environmental Damage Accumulation Metric (EDAM). The form of this metric is through a Box-Lucas asymptote type expression as:

$$b = b_{\mathrm{REF}} + c \cdot (1 - e^{-\xi \cdot t}), \tag{2}$$

where b_{REF} is the value of parameter b for dry specimens marked REF, t is the time in months and c and ξ are constants obtained by curve fitting. At time 0 then $b = b_{\mathrm{REF}}$. In theory the maximum possible value of the parameter b should not be more than 1, since a contradiction to that would mean energy is created. On Fig. 12 some results at from specimens immersed at 65 °C go over that value. The reason for this could be explained by the slight penetration and the calculation error involved and finally the error introduced by normalization. The impact

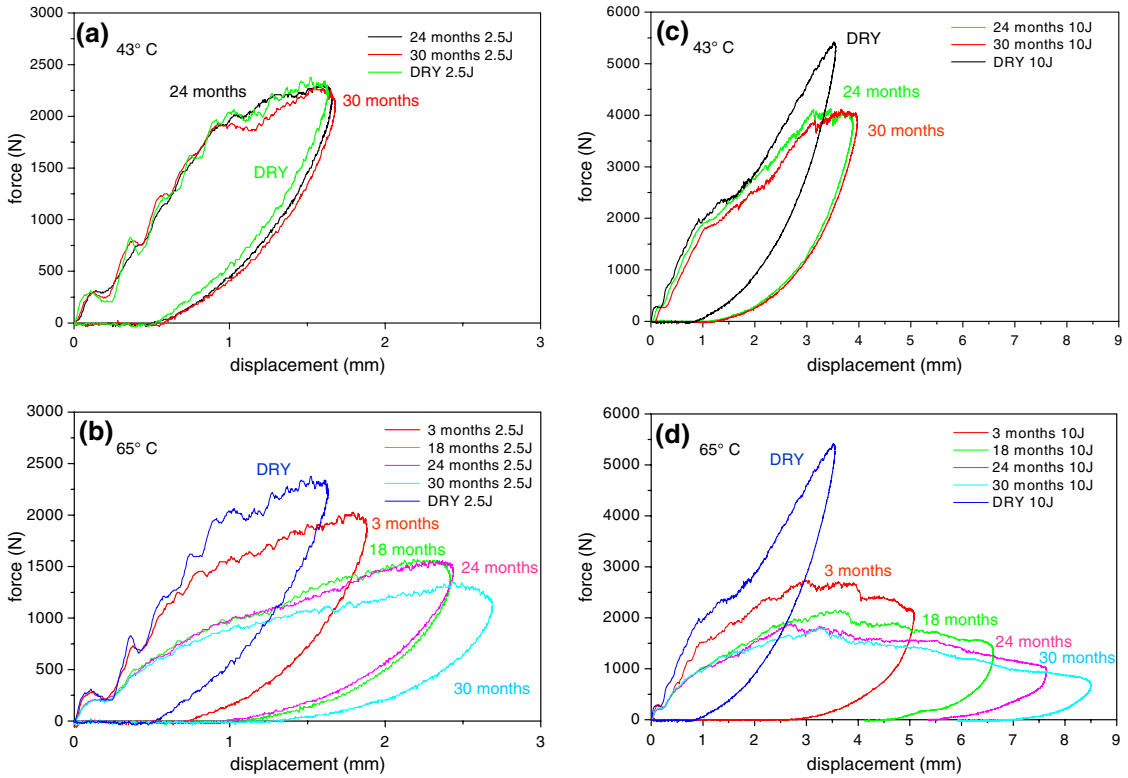

Fig. 9 Force–displacement diagrams from impacts on material type A. Specimens marked DRY were impacted when dry. Specimens were impacted after water immersion at 43 °C, in (**a**) and (**c**). Specimens were impacted after water immersion at 65 °C in (**b**) and (**d**), for a period equal to the number printed in months

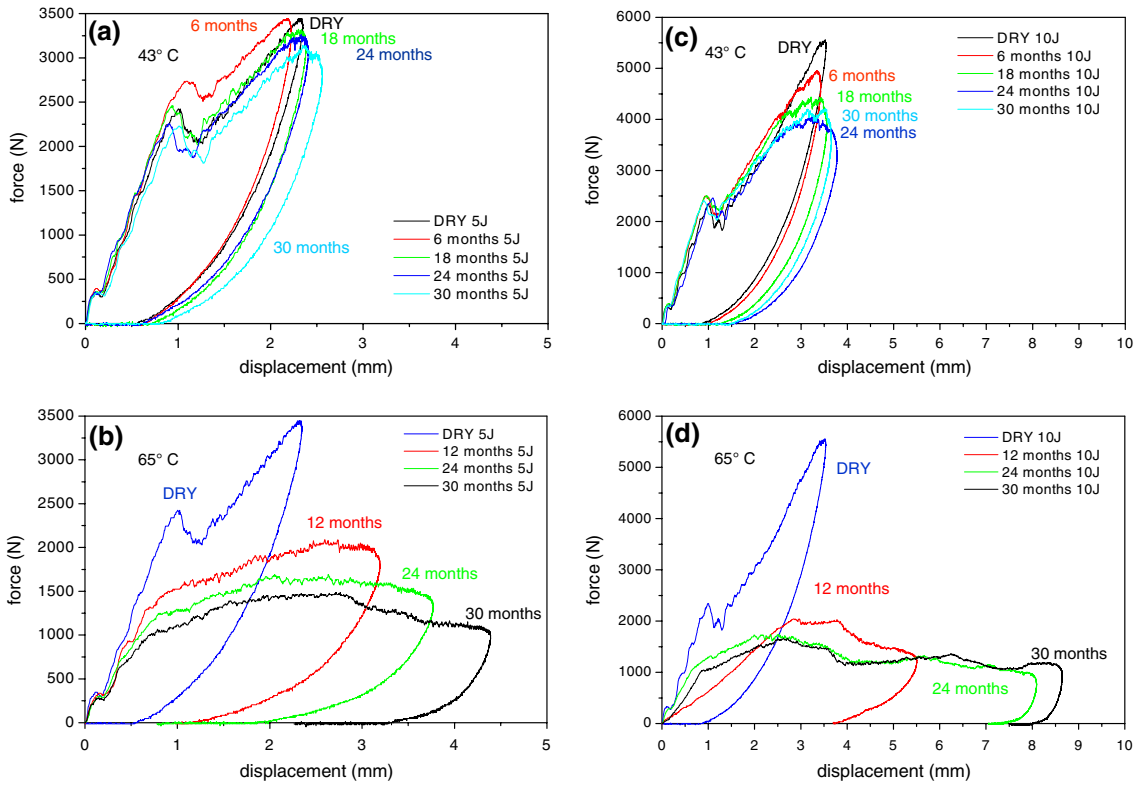

Fig. 10 Force–displacement diagrams from impacts on material type B. Specimens marked DRY were impacted when dry. Specimens were impacted after water immersion at 43 °C, in (**a**) and (**c**). Specimens were impacted after water immersion at 65 °C in (**b**) and (**b**), for a period equal to the number printed in months

energy used for normalization is a nominal value and it is possible that the starting energy is slightly higher than the nominal. This problem arises due to the height adjustment system of the drop weight tower not being very precise.

Another perspective on the effects of prolonged water immersion on the impact resistance behaviour of the materials can be obtained by plotting force against time. The change in behaviour for impact at same energy level of 10 J after different water immersion periods is presented in Fig. 13 for material type D.

A gradual change in behaviour is marked on the curves in Fig. 13. For clarity not all time sets tested have been plotted, but clearly these show the trends. Longer water immersion time reduced the peak load. The duration of the impact event is also increasing with time of immersion. This relates mainly to increased compliance, the cause of which can mainly be attributed to the interface degradation.

Discussion

Water immersion causes mass changes to composites. A fast increase in mass is recorded first due to water absorption. The rate of this increase is temperature controlled and increasing with temperature. After this initial part, at 43 °C a much slower increase in mass was recorded. At 65 °C a multi-stage diffusion was encountered. At some stage around 14 months after the start, a relatively fast mass loss was recorded. The turning point signifies the point where the specimen mass loss due to dissolution becomes the dominant mechanism over the water uptake. It has to be considered then that after an initial incubation period the mass loss mechanism was activated, before the turning point revealed at 14 months. Since a single series of specimens were used to follow the water diffusion it was not possible to recover information about the exact initiation time and rate of mass loss through drying of specimens. Weight loss has been exhibited and presented in other resin/fibre systems [11].

An assumption was made regarding the linearity of the relationship between impact energy and absorbed energy. Results have shown this assumption to hold for the range of impact energies tested. As a result of this observation EDAM was formulated, that relates the change of slope of the ratio of the absorbed impact energy with the initially given impact energy, over time. It is seen that parameter b follows a time-dependent path, whose trend can be described with a Box-Lucas type exponential curve.

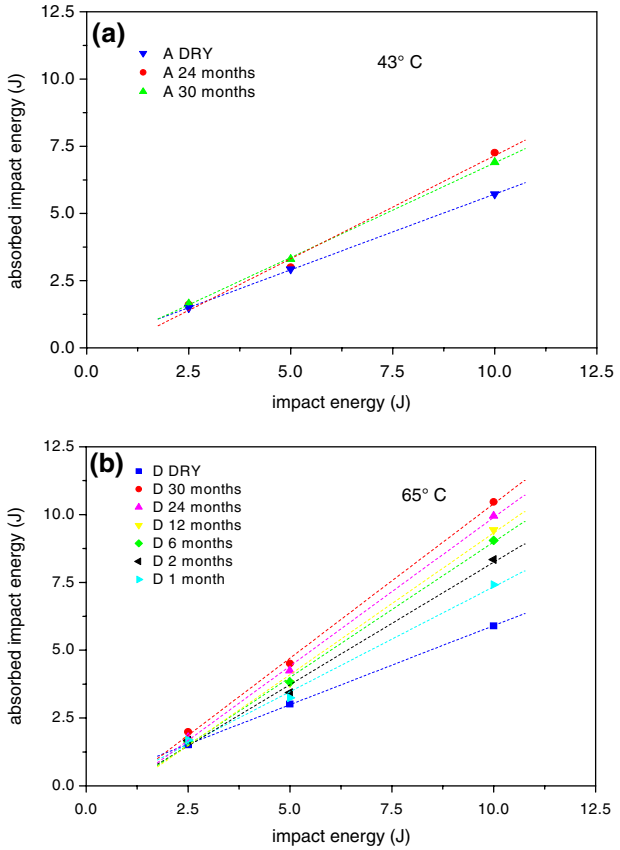

Fig. 11 Absorbed impact energy against nominal impact energy for material type A in (**a**) and type D in (**b**). Specimens impacted dry are marked DRY in (**a**) and (**b**). Numbers correspond to months of immersion in water at 43 °C in (**a**) and at 65 °C in (**b**). Dotted lines are the respective best linear fits

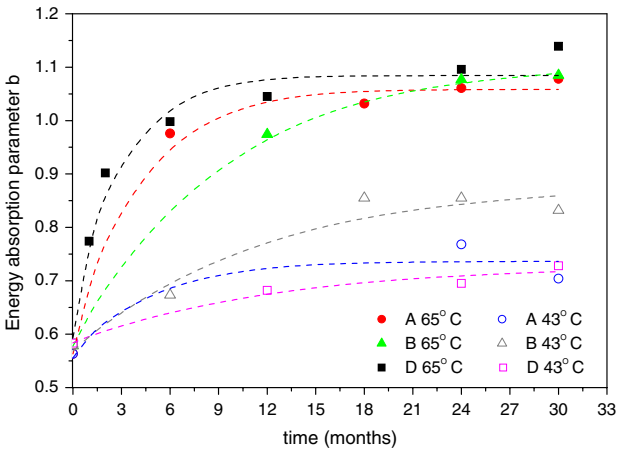

Fig. 12 The energy absorption parameter b against time for all types of specimens A, B and D at temperatures of 43 and 65 °C

Regardless of the material type the initial value of b is close to 0.55 and in time reaches over 1, where specimen penetration takes place. The trend was primarily followed at 65 °C. The trend holds for immersion at 43 °C but the change-over for b to a value over 1 might not be encountered.

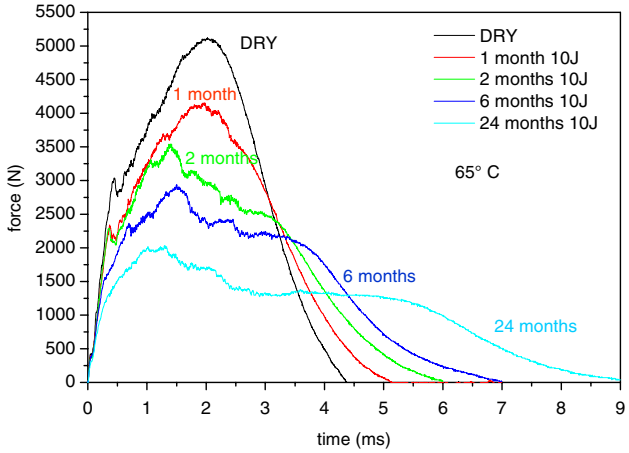

Fig. 13 Force–time plot for material type D impacted at 10 J as DRY and after water immersion at 65 °C for the duration marked in months

The material changes witnessed in terms of water uptake can be linked with what was observed in terms of impact energy absorption. The EDAM parameter b can be considered a measure of the ability of a material to perform elastically under impact. For values of the parameter b less than 1, the material behaves still, partially at least, in an elastic manner. For values of the parameter b higher than 1, specimen penetration is achieved and no energy is returned to the striker. A close observation at the time line in Fig. 12 for material type D at 65 °C, which is the most complete curve at that temperature, reveals that the change-over to values over 1 happens some time between months 7 and 12, of water immersion. It is significant that is just prior to the point where the weight change slope becomes negative, at about 14 months after start.

Conclusion

The present study has attempted to show a link between water immersion and its effects on impact response of composites plates. The accelerating effect of increased water temperature immersion was reaffirmed. Impact damage on plates immersed in water did not significantly differentiate their absorption characteristics at any immersion temperature. Neat resin plates showed significantly higher initial absorption rates and temporary plateaus when compared to their respective composite plates. Based on this finding, it was considered normal that the two NCF glass reinforced materials B and D showed higher water absorption levels, since they had the lower V_f % when compared to the woven type A material.

The study accounted for differences encountered in terms of peak impact force and impact energy absorption.

Water immersion considerably lowered peak impact force over time of immersion. Energy absorption on the other hand increased over time as the lower peak impact force encountered was compensated by increased deflection and partial or complete indentation allowed due to the degraded state of the material. Based on this finding a semi-empirical Environmental Damage Accumulation Metric (EDAM) was proposed. A change-over point in time is suggested by the data where complete loss of elastic behaviour of the plate is encountered.

References

1. Bank LC, Gentry TR, Barkatt A (1995) J Reinforced Plastics Compos 14:559
2. Weitsman Y (2000) Comprehensive composite materials. Elsevier, New York, p 369
3. Schutte CL (1994) Mater Sci Eng R13:265
4. Springer GS, Sanders BA, Tung RW (1980) J Compos Mater 14:213
5. Boinard E, Pethrick RA, Dalzel-Job J, MacFarlane CJ (2000) J Mater Sci 35:1931
6. Tsotsis TK, Lee SM (1997) J Reinforced Plastics Compos 16:1609
7. Pavlidou S, Papaspyrides CD (2003) Composites Part A 34A:1117
8. Benameur T, Granger R, Vergnaud JM (1995) Polymer Test 14:35
9. Ciriscioli PR, Lee WI, Peterson DG, Springer GS, Tang J (1987) J Compos Mater 21:225
10. Ashbee KHG, Wyatt RC (1969) Proc Roy Soc 312:553
11. Perreux D, Choqueuse D, Davies P (2002) Composites Part A 33:147
12. Belan F, Bellenger V, Mortaigne B, Verdu J, Yang YS (1996) Compos Sci Technol 56:733
13. Abrate S (1991) Appl Mech Rev 44:155
14. Abrate S (1994) Appl Mech Rev 47:517
15. Cantwell WJ, Morton J (1991) Composites 22:347
16. Richardson MO, Wisheart MJ (1996) Composites Part A 27:1123
17. Shoeppner GA, Abrate S (2000) Composites Part A 31:903
18. Qi B, Herszberg I (1999) Compos Struct 47:483
19. Strait LH, Karasek ML, Amateau MF (1992) J Compos Mater 26:2118
20. Komai K, Minoshima K, Yamasaki H (1995) In: 1st International conference on mechanics of time dependent materials, Ljubljana
21. Berketis K (2006) Water immersion and impact damage effects on the residual compressive strength of composites. Materials Department, Queen Mary, University of London, London
22. Lundgren JE, Gudmundson P (1999) Compos Sci Technol 59:1983